

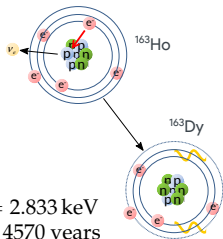
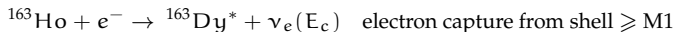
Status of HOLMES, an experiment for measuring the neutrino mass

Elena Ferri

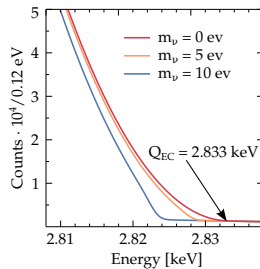
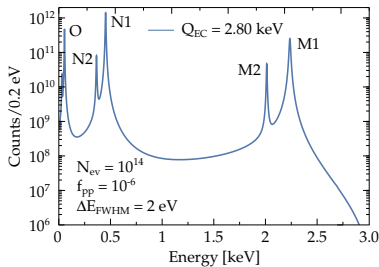
*INFN of Milano-Bicocca
on behalf of HOLMES collaboration*



^{163}Ho Electron Capture for measuring the neutrino mass



$Q_{\text{EC}} = 2.833 \text{ keV}$
 $\tau_{1/2} \simeq 4570 \text{ years}$



- Calorimetric measurement of Dy atomic de-excitations (mostly non-radiative)

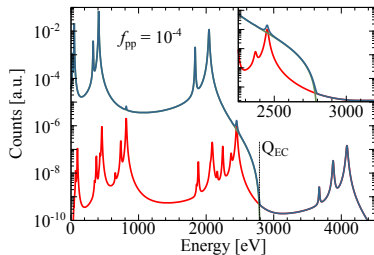
⇒ measurement of the entire energy released except the ν energy

- rate at the end point depends on $(Q - E_{M1})$: the proximity to M1 resonance peak enhances the statistics at the end point (i.e. sensitivity on m_ν)
- Searching for a tiny deformation caused by a non-zero neutrino mass to the spectrum near its end point

proposed for the first time
by A. De Rujula e M. Lusignoli in 1982
Phys. Lett. 118B (1982) 429
Nucl. Phys. B219 (1983) 277-301



$$S(E_c) = [N_{ev}(N_{EC}(E_c, m_v) + f_{pp} \times N_{EC}(E_c, 0) \otimes N_{EC}(E_c, 0)) + B(E_c)] \otimes R_{\Delta E}(E_c)$$



N_{ev}	: total number of events
$N_{EC}(E_c, m_v)$: ^{163}Ho spectrum
$B(E)$: background energy spectrum
$R_{\Delta E}(E_c)$: detector energy response function
f_{pp}	: fraction of pile-up events
$R_{\Delta E}(E_c)$: detector energy response function
ΔE	: interval of energy

more details on

[Eur. Phys. J. C 74 \(2014\) 3161](#)

- Pulse pile-up occurs when multiple events arrive within the temporal resolving time of the detector
- Unresolved pile-up events close to the end-point impairing effect on the end-point measurement
- The ^{163}Ho pile-up events spectrum is quite complex and presents a number of peaks at the end-point
- To resolve pile-up:
 - Detector with fast signal rise-time τ_{rise}
 - Pile-up recognition algorithm (i.e. Wiener filter, Singular Value Decomposition)



The m_ν statistical sensitivity has:

- **Strong** dependence on statistic: $\Sigma(m_\nu) \propto N_{\text{events}}^{1/4}$
- **Strong** dependence on pile-up: $f_{\text{pp}} \simeq A_{\text{EC}} \cdot \tau_{\text{res}}$
(A_{EC} : pixel activity, τ_{res} : time resolution)
- **Weak** dependence on energy resolution ΔE ;

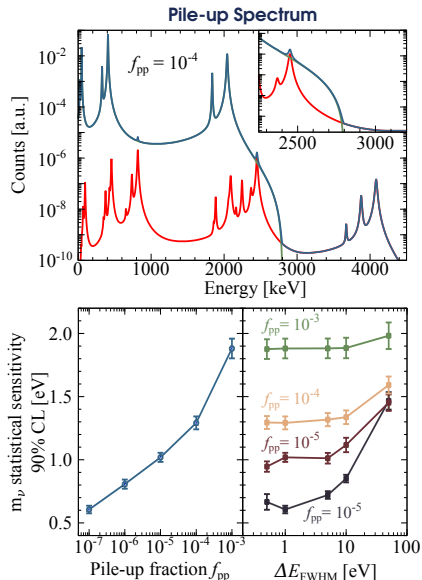
Multiplexable detectors with fast response are required

HOLMES

Neutrino mass determination with a sensitivity as low as ≈ 1 eV

- Microcalorimeters based on Transition Edge Sensors with ^{163}Ho implanted Au absorber
- Pixel activity of $A_{\text{EC}} \sim 300$ Bq/det
- Energy resolution: $O(\text{eV})$
- Time resolution: $\tau_{\text{res}} \sim 3 \mu\text{s}$ ($\tau_{\text{rise}} = 10 - 20 \mu\text{s}$);
- 1000 channels for $3 \cdot 10^{13}$ events collected in $T_M = 3$ years

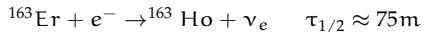
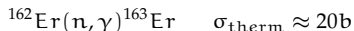
more details on
Eur. Phys. J. C (2015) 75: 112



^{163}Ho production and chemical purification

Production

^{163}Ho production from ^{162}Er neutron activation



- ^{162}Er irradiation at ILL nuclear reactor @ Grenoble: high thermal n flux
- cross section burn up $^{163}\text{Ho}(n, \gamma)^{164}\text{Ho}$ not negligible ($\sim 200\text{b}$)
- $^{165}\text{Ho}(n, \gamma)^{166\text{m}}\text{Ho}$ ($\beta, \tau_{1/2} \sim 1200\text{y}$) from Ho contamination or ^{164}Er

Tm 163 1.81 h $\epsilon^- \beta^+ \dots$ γ 104; 69; 241; 1454; 1397	Tm 164 5.1 m 2.0 m $\epsilon^- \beta^+ \dots$ γ 208; 315...	Tm 165 30.06 h $\epsilon^- \beta^+ \dots$ γ 243; 47; 287; 607...	Tm 166 7.70 h $\epsilon^- \beta^+ 1.9 \dots$ γ 779; 2052; 184; 1274...	Tm 167 9.25 d $\epsilon^- \gamma$ 532... m	Tm 168 93.1 d $\epsilon^- \beta^+ \dots$ γ 198; 816; 447...
Er 162 0.139 α 19 $\sigma_{n, \alpha} < 0.011$	Er 163 75 m $\epsilon^- \beta^+ \dots$ γ (1114...) g	Er 164 1.601 α 13 $\sigma_{n, \alpha} < 0.0012$	Er 165 10.3 h ϵ^- no γ	Er 166 33.503 α 3 + 14 $\sigma_{n, \alpha} < 7\text{E-}5$	Er 167 2.3 s 22.869 β^- 208 $\sigma_{n, \alpha} 3\text{E-}6$
Ho 161 6.7 s 2.5 h $\epsilon^- \gamma$ 26; 78; 211	Ho 162 68 m 15 m $\epsilon^- \beta^+ \dots$ γ 165; 36... 220; 283; 1319; 957...	Ho 163 1.1 s 4570 s ϵ^- no γ	Ho 164 37 m 29 m $\epsilon^- \beta^+ \dots$ γ 37; 57; 73...	Ho 165 100 α 3.1 + 58 $\sigma_{n, \alpha} < 2\text{E-}5$	Ho 166 1200 a 26.80 h 2.07... β^- 19... 810; 712 γ 81... σ 3100
Dy 160 2.329 α 60 $\sigma_{n, \alpha} < 0.0003$	Dy 161 18.889 α 600 $\sigma_{n, \alpha} < 1\text{E-}6$	Dy 162 25.475 α 170	Dy 163 24.896 α 120 $\sigma_{n, \alpha} < 2\text{E-}5$	Dy 164 28.260 α 1610 + 1040	Dy 165 1.3 m 2.35 h β^- 106; ϵ^- β^- 9.9; 1.3... 1.6... γ 195; 515... (262...) σ 3000
Tb 159 100	Tb 160 72.3 d	Tb 161 6.80 d	Tb 162 7.78 d	Tb 163 18.5 m	Tb 164 2.0 m

Purification

Chemical purification @ PSI before and after the irradiation

- radiochemical separation with ion-exchange chromatography
- efficiency better than 79%
- Expected $^{166\text{m}}\text{Ho}$ contamination fraction: $\sim 10^{-3}$

Sample processed

Enriched Er_2O_3 samples irradiated @ ILL, pre and post processed @ PSI:

- 25 mg, 55 days irradiation, $A(^{163}\text{Ho}) \sim 5\text{ MBq}$
- 150 mg, 53 days irradiation, $A(^{163}\text{Ho}) \sim 38\text{ MBq}$
- 544 mg, 50 days irradiation, $A(^{163}\text{Ho}) \sim 120\text{ MBq}$
- * $\sim 100\text{ MBq}$ enough for R&D and 500 pixels



Ion implanter designed to embed Ho inside the detectors absorbers and to perform a mass separation of the ^{163}Ho from the other contaminants.

- extraction voltage 30-50 kV \rightarrow 10-100 nm implant depth
- $^{163}\text{Ho}/^{166\text{m}}\text{Ho}$ separation better than 10^5

Au co-evaporation:

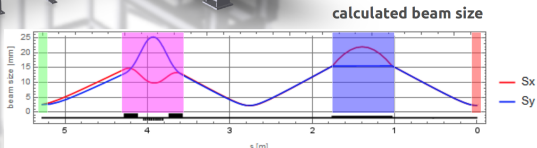
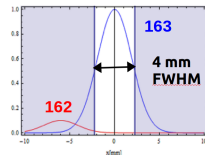
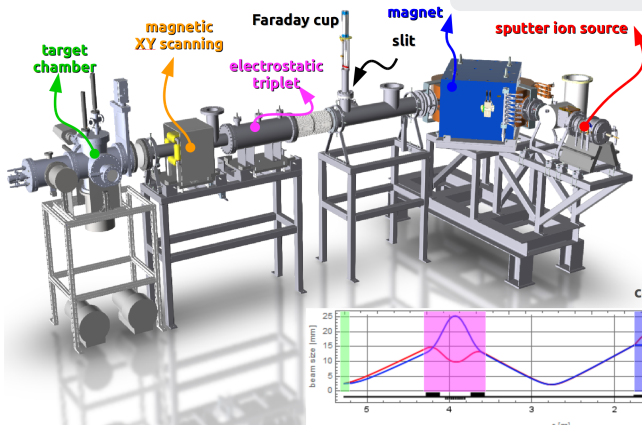
- to fully encapsulate the source
- to compensate the saturation of the ^{163}Ho concentration in the absorber
- to avoid oxidation
- heat capacity

Target chamber:

- 4 COMIC microwave sources
 - 4 Ar beams hit on 4 Au targets
- \rightarrow 4 in order to increase the deposition rate and uniformity

Main components:

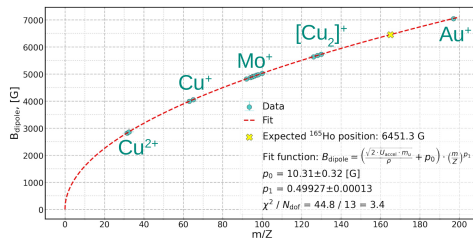
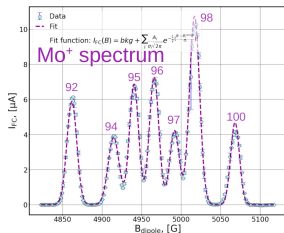
- Ar penning sputter ion source
- magnetic dipole mass analyzer ($B_m \propto x = 1 \text{ T}$)
- faraday cup and slit
- target chamber for Au co-evaporation



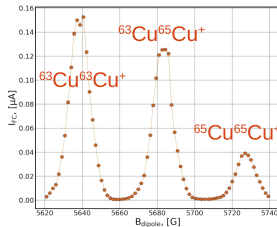
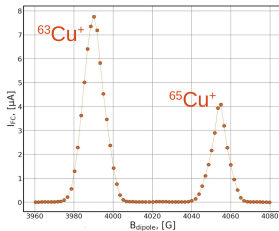
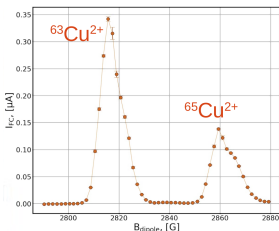
Ion implanter calibration



Magnetic field vs mass-to-charge ratio calibration with Cu, Au and Mo peaks.



- Cu/Au from sputter target/holder
- Mo from the anode
- The source produces also multiple-ionized and dimeric ions from the same material, which can also be used for calibration



for more details
 Mariia Fedkevych's talk @ NuMass 2022

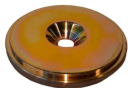


Efforts are put to build the most suitable target for the Ho sputtering

→ different techniques for target fabrication are tested

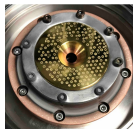
Molecular plating

Electrodeposition of Ho complexes in an organic solvent at high voltages with high uniformity and efficiency (>90%)



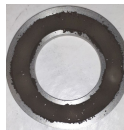
Drop-on-demand inkjet printing

put droplets of solution containing compound and let solvent evaporate to deposit the dissolved compound



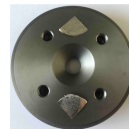
Sintered targets

$\text{Ho}(\text{NO}_3)_3$ in a metallic mixture of Zr and Y fine-grained powder prepressed at 350 bar/cm² and baked at 950°C

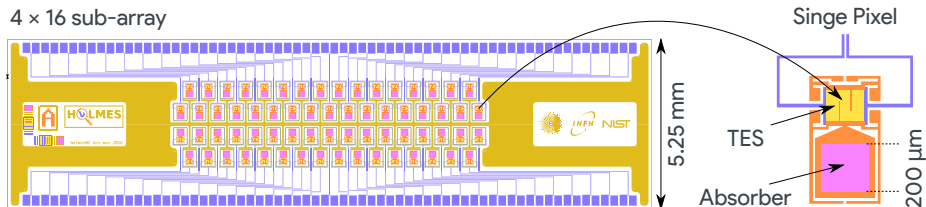


Coupled reduction

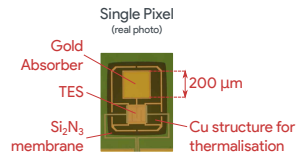
Ho reduction and diffusion into backing material due to thermodynamically favourable formation of intermetallic compound



With **sintered target** we obtained the best current-stability: O(200) nA over 15 h!



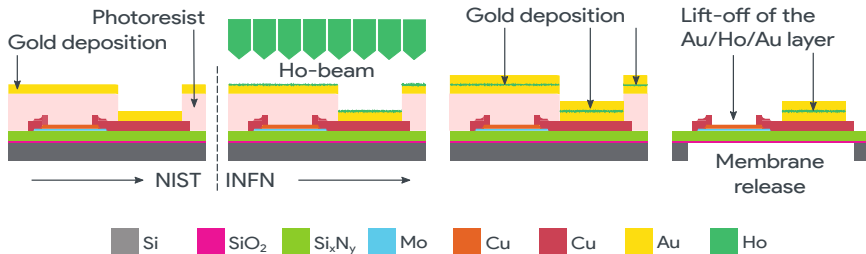
- Mo/Cu TES coupled to Gold absorbers where ^{163}Ho will be ion-implanted
- $2\text{ }\mu\text{m}$ Gold thickness for full e/γ absorption
- Side-car design to avoid TES proximitation effect
- Thermal conductance G engineering for τ_{decay} control
- 4×16 linear sub-array designed for high implant efficiency and low parasitic L
- **Optimized design for high speed and high resolution:**



Specs @ 2.8 keV : $\Delta E_{\text{FWHM}} \simeq 3 - 4\text{ eV}$, $\tau_{\text{rise}} \simeq 10\text{ }\mu\text{s}$, $\tau_{\text{decay}} \simeq 100\text{ }\mu\text{s}$



^{163}Ho isotopes embedded in metallic absorbers (through ion-implantation)



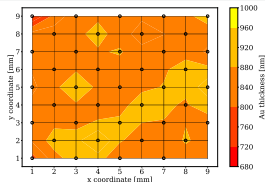
- Fabrication in two steps:
 - NIST: TES fabrication with 1 μm Au absorber
 - INFN: ^{163}Ho implantation, final deposition of 1 μm Au and SiN membrane release
- final micromachining step definition in progress
 - ⇒ KOH vs DRIE machining

HOLMES: detectors fabrication process (cont.)

Au deposition

1 μm of Au deposited

- with Ion beam sputter system
- at rate of around 52 nm/h
→ about 20 h for 1 μm
- gold thickness uniformity
→ $\sigma_t/t \sim 4\%$



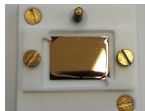
Lift-off

Removal of the resist mask (7 μm thickness)

- sample in acetone at 40°C for 24 h

After the lift-off, the Au deposited remains only on the absorber:

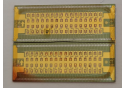
→ Minimal crowning and almost isotropical deposition thanks to the 4 ion beam sources



Au removed with the lift-off



Arrays after the lift-off



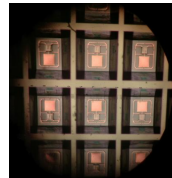
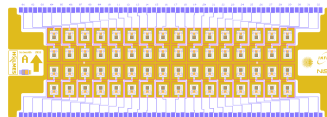
Zoom of a single absorber



Membrane release

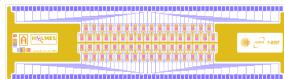
KOH

- Anisotropic wet etching
- Requires more spacing between pixels
- Successfully tested

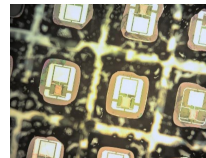


DRIE

- Silicon Deep Reactive Ion Etching
- Best for close packing
- High implant efficiency
- Not yet tuned

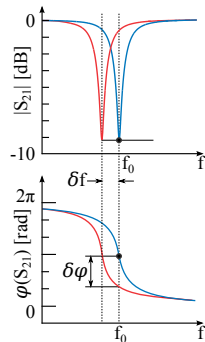
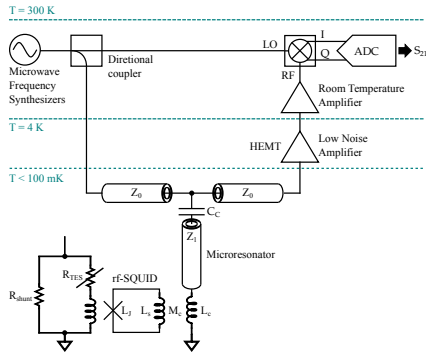


calculated ^{10}B beam FWHM width



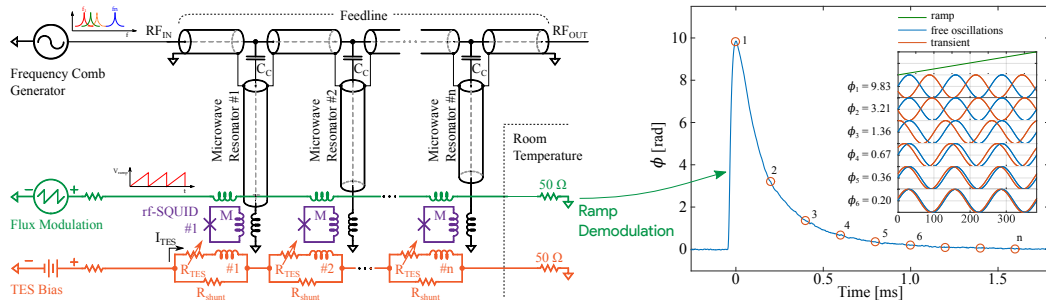


HOLMES TESs readout is based on microwave rf-SQUID multiplexing



- rf-SQUID inductively coupled to a dc-biased TES and to a high-Q superconducting $\lambda/4$ -wave resonator
- Change in TES current \Rightarrow change in the input flux to the SQUID
- The rf-SQUID transduces a change in input flux into a variation of resonant frequency and phase
- Each micro-resonator can be continuously monitored by a probe tone

Microwave rf-SQUID multiplexing (cont.)

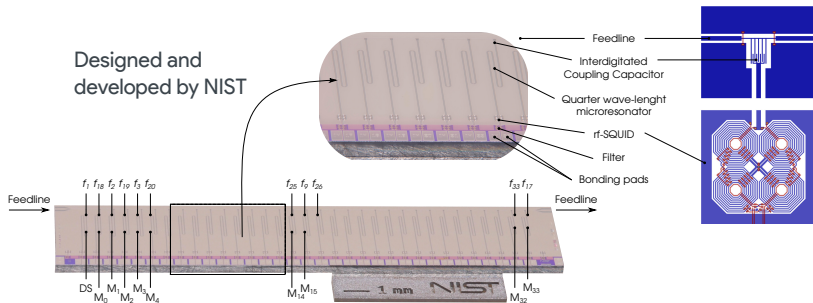


- By coupling many resonators to a single microwave feedline it is possible to readout multiple detectors
- Sensors are monitored by a set of sinusoidal probe tones (frequency comb)
- At equilibrium, the resonator frequencies are matched to the probe tone frequencies, and so each resonator acts as a short to ground
- The ramp induces a controlled flux variation in the rf-SQUID, which is crucial for linearizing the response
- Large multiplexing factor (> 100) and bandwidth, **currently limited by the digitizer bandwidth**

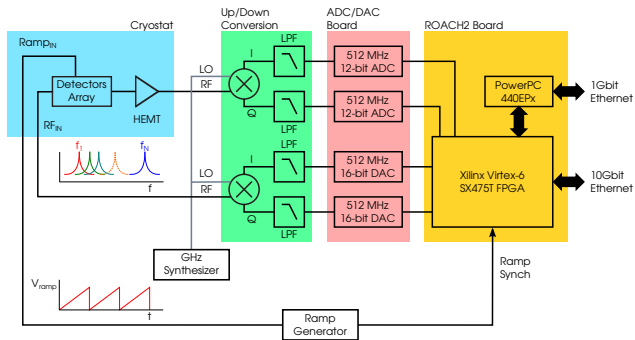
The Multiplexing chip



The core of the microwave multiplexing is the **multiplexer chip**



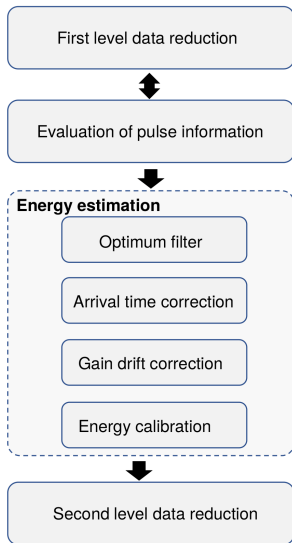
- Superconducting 33 quarter-wave coplanar waveguide (CPW) microwave resonators covering 500 MHz in the 4-8 GHz frequency range
- 200 nm thick Nb film deposited on high-resistivity silicon ($\rho > 10 \text{ k}\Omega \cdot \text{cm}$)
- each resonator has a trombone-like shape with slightly different length
- 2 MHz bandwidth per resonator
- separation between resonances 14 MHz (to prevent cross-talk)
- resonance depth greater than 10 dB
- squid equivalent noise less than $2\mu\phi_0 / \sqrt{\text{Hz}}$



- Software Defined Radio with the open system ROACH2 (Casper collaboration)
- ADC BW 550 MHz
- real time pulse reconstruction
→ at the moment readout available for 64 channels

Multiplexing factor proportional to the target rise time

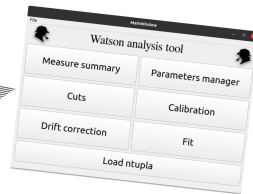
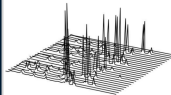
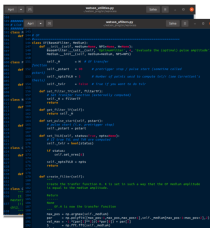
- $n_{\text{TES}} \approx 3.4 \cdot \tau_{\text{rise}}$
- requiring $\tau_{\text{rise}} = 10\mu\text{s}$



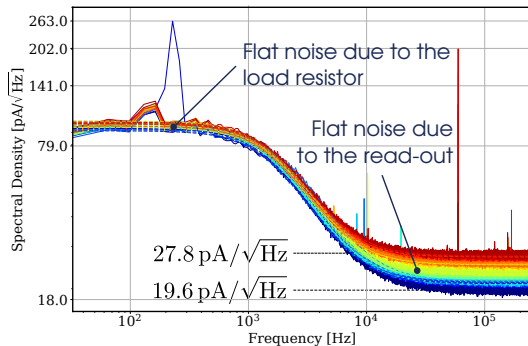
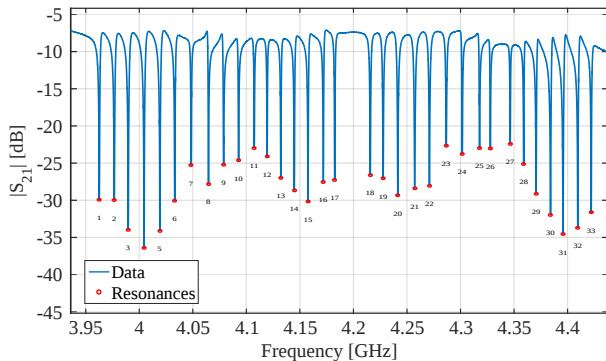
- Robust analysis is mandatory for achieving the expected microcalorimeter intrinsic energy resolution.
- The data from each pixel need to be processed separately.

Watson toolkit

- Software for low temperature detector data analysis
- Object oriented programming. Written in python (numpy and scipy)
- Fast, easy to read, easy to fix code
- GUI with QT5 for handy day to day operations
- Data are stored in hdf5 (hierarchical, filesystem-like data format)



Multiplexing: characterization results



		Required	Measured
Resonators bandwidth	Δf_{BW} [MHz]	2	2 ± 1
Resonators spacing	Δf [MHz]	14	14 ± 1
Resonators depth	ΔS [dB]	> 10	29 ± 6

All the microresonator parameters match the HOLMES specification

Improved read out noise

$$\rightarrow n_s = (23 \pm 2) \text{ pA} / \sqrt{\text{Hz}}$$

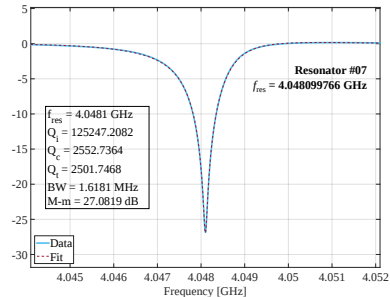
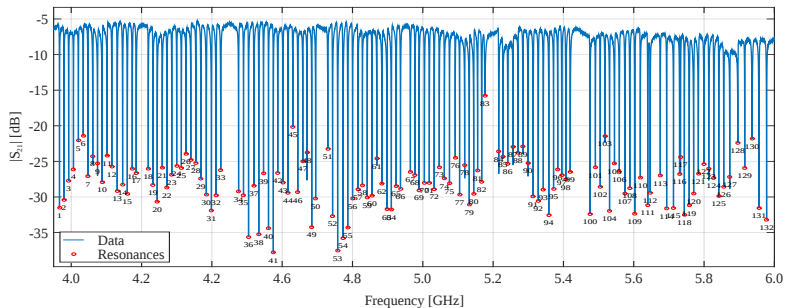
Previous work

$$\rightarrow n_s = (26 \pm 7) \text{ pA} / \sqrt{\text{Hz}}$$

more details on
IEEE TAS 31 (2021) 5, 2100205

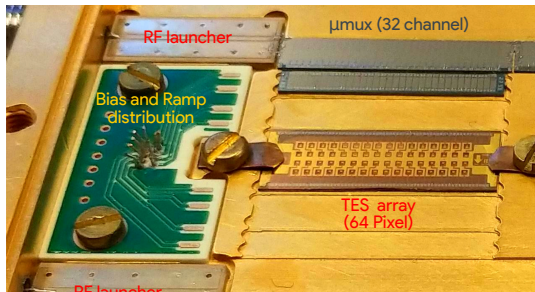
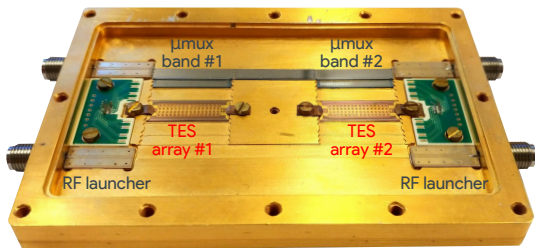


Forward transmission S_{21} of 4 different band chips wired in series and an example of resonance fit

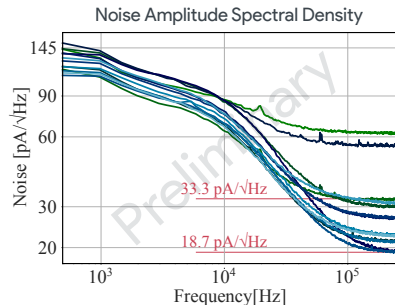
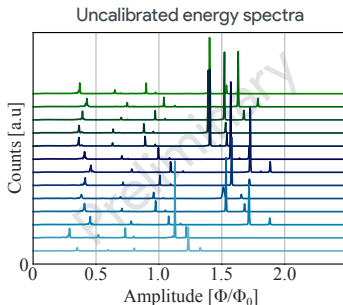
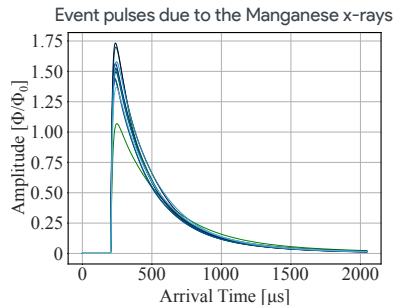


Four μ mux in series are able to cover a wide frequency range from 4 to 6 GHz

HOLMES: test on the processed detectors



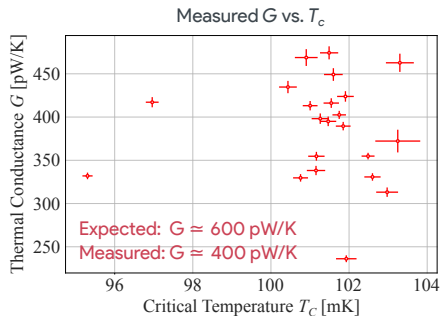
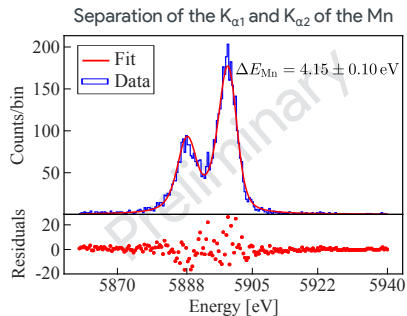
- Holder designed to host 128 Channels:
 - ▶ $2 \times (4 \times 16)$ sub arrays
 - ▶ $4 \times \mu\text{mux}$ multiplexer chips with 4 bands
- 8 holders will cover the entire HOLMES in its final configuration (1024 channels);
- Preliminary low temperature tests performed with **fully processed arrays** (with KOH):
 - ▶ detector with (1 μm) absorber at NIST
 - ▶ absorber finalized (1 μm) at MIB
 - ▶ wet etching at MIB
- **32+32 TES pixels bonded** (half of the available)
- Absorbers without the ^{163}Ho implanted
- New SDR firmwares for 16 and 32 channels:
 - 16-channel version fully operational
 - 32-channel version under testing
- New up/down-conversion system fully operational



- **non implanted detectors** with KOH membrane release
- 13/16 working detectors (3 detectors with problematic resonators)
- Calibration run performed with a primary ^{55}Fe source faced to different targets
- Calibration lines:
 ^{55}Mn (5.9 keV) ^{40}Ca (3.7 keV) ^{40}Cl (2.6 keV) ^{27}Al (1.5 keV)

Measured read out noise
 $n_s \sim (19 - 33) \text{ pA}/\sqrt{\text{Hz}}$

- Compatible with the previous prototypes
Eur. Phys. J. C (2019) 79:304
- Two channels with higher noise due to not optimal rf-SQUID oscillations



For the best detector: $\Delta E_{Mn} = 4.15 \pm 0.10 \text{ eV} @ 5.9 \text{ keV}$

- Energy resolution in the (4 - 6) eV range @ 5.9 keV
Large spread probably due to the large G dispersion
different $G \Rightarrow$ different working point
- $\tau_{\text{rise}} \simeq 20 \mu\text{s}$ and $\tau_{\text{fall}} \simeq 300 \mu\text{s}$
longer fall time due to lower thermal conductance G

KOH vs DRIE machining

- same energy resolution and rise time
- longer decay time and larger coupling dispersion



The count rate at the ROI is very low (0.26 counts/eV/day/det @ [2650,2833]eV)

→ the fraction of background signals must be kept as low as possible

Background

1. Pile-up

→ the main background source for pixel with $A_{EC} \sim 300$ Bq and $\tau_R \sim 1.5$ μ s. (0.8 counts/eV/day/det @ ROI)

2. Internal radionuclides

^{166m}Ho → expected count rate < 0.01 counts/eV/day/det @ ROI

3. Natural radioactivity

Smooth and almost flat background @ ROI except for ^{40}K

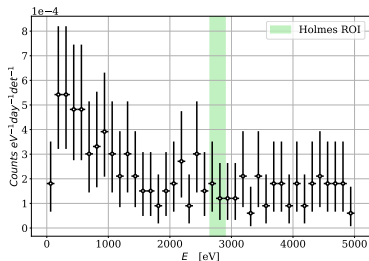
4. Cosmic rays

GEANT 4 simulation 5×10^{-5} counts/eV/day/det @ [0,4000] eV

3. and 4. can be comparable or even overcome the pile-up rate if the ^{163}Ho activity per pixel is too low.

Background measurement

Single interaction in a pixel produces a background spectrum which seems to be monotonically decreasing.



0.0001 counts/eV/day/det @ HOLMES ROI

→ lowering with a muon veto



- A powerful tool to determine the effective electron-neutrino mass is the calorimetric measurement of the energy released in ^{163}Ho electron capture (EC)
- The HOLMES experiment will perform a direct measurement of the neutrino mass by using TES microcalorimeters
- Ion implanter is working as expected. The production of a proper sputter target is almost ready!
- The software for analysis and signal processing of microcalorimeters events is up and running!
- For reading out the 1024 detectors, HOLMES will use the microwave multiplexing read-out
 - All the microresonator parameters match the HOLMES specification
- Transition edge sensors with Au absorber where the ^{163}Ho will be ion-implanted
 - Tested and tuned the final array fabrication processes
 - TES characterization with a fluorescence source without Ho
 - The performances (energy and time resolution) required by HOLMES are achieved
- The first phase of the HOLMES experiment is expected on the last quarter of 2022: a low dose implantation of a 2×32 pixel array